Parasites & Vectors

RESEARCH Open Access

RNA sequencing reveals dynamic expression of lncRNAs and mRNAs in caprine endometrial epithelial cells induced by *Neospora caninum* infection

Shan-Shan Zhao[1], De-Liang Tao[1], Jin-Ming Chen[1], Jiang-Ping Wu[1], Xin Yang[1], Jun-Ke Song[1], Xing-Quan Zhu[2,3*] and Guang-Hui Zhao[1*]

Abstract

Background: The effective transmission mode of *Neospora caninum*, with infection leading to reproductive failure in ruminants, is vertical transmission. The uterus is an important reproductive organ that forms the maternal–fetal interface. *Neospora caninum* can successfully invade and proliferate in the uterus, but the molecular mechanisms underlying epithelial-pathogen interactions remain unclear. Accumulating evidence suggests that host long noncoding RNAs (lncRNAs) play important roles in cellular molecular regulatory networks, with reports that these RNA molecules are closely related to the pathogenesis of apicomplexan parasites. However, the expression profiles of host lncRNAs during *N. caninum* infection has not been reported.

Methods: RNA sequencing (RNA-seq) analysis was used to investigate the expression profiles of messenger RNAs (mRNAs) and lncRNAs in caprine endometrial epithelial cells (EECs) infected with *N. caninum* for 24 h (TZ_24h) and 48 h (TZ_48 h), and the potential functions of differentially expressed (DE) lncRNAs were predicted by using Gene Ontology (GO) enrichment and Kyoto Encyclopedia of Genes and Genomes (KEGG) analysis of their mRNA targets.

Results: RNA-seq analysis identified 1280.15 M clean reads in 12 RNA samples, including six samples infected with *N. caninum* for 24 h (TZ1_24h-TZ3_24h) and 48 h (TZ1_48h-TZ3_48h), and six corresponding control samples (C1_24h-C3_24h and C1_48h-C3_48h). Within the categories TZ_24h-vs-C_24h, TZ_48h-vs-C_48h and TZ_48h-vs-TZ_24h, there were 934 (665 upregulated and 269 downregulated), 1238 (785 upregulated and 453 downregulated) and 489 (252 upregulated and 237 downregulated) DEmRNAs, respectively. GO enrichment and KEGG analysis revealed that these DEmRNAs were mainly involved in the regulation of host immune response (e.g. TNF signaling pathway, MAPK signaling pathway, transforming growth factor beta signaling pathway, AMPK signaling pathway, Toll-like receptor signaling pathway, NOD-like receptor signaling pathway), signaling molecules and interaction (e.g. cytokine-cytokine receptor interaction, cell adhesion molecules and ECM-receptor interaction). A total of 88 (59 upregulated and 29 downregulated), 129 (80 upregulated and 49 downregulated) and 32 (20 upregulated and 12 downregulated)

*Correspondence: xingquanzhu1@hotmail.com; zgh083@nwsuaf.edu.cn

[1] College of Veterinary Medicine, Northwest A&F University, Yangling 712100, Shaanxi, China
[2] College of Veterinary Medicine, Shanxi Agricultural University, Taigu 030801, Shanxi, China
Full list of author information is available at the end of the article

DElncRNAs were found within the categories TZ_24h-vs-C_24h, TZ_48h-vs-C_48h and TZ_48h-vs-TZ_24h, respectively. Functional prediction indicated that these DElncRNAs would be involved in signal transduction (e.g. MAPK signaling pathway, PPAR signaling pathway, ErbB signaling pathway, calcium signaling pathway), neural transmission (e.g. GABAergic synapse, serotonergic synapse, cholinergic synapse), metabolism processes (e.g. glycosphingolipid biosynthesis-lacto and neolacto series, glycosaminoglycan biosynthesis-heparan sulfate/heparin) and signaling molecules and interaction (e.g. cytokine-cytokine receptor interaction, cell adhesion molecules and ECM-receptor interaction).

Conclusions: This is the first investigation of global gene expression profiles of lncRNAs during *N. caninum* infection. The results provide valuable information for further studies of the roles of lncRNAs during *N. caninum* infection.

Keywords: *Neospora caninum*, Caprine endometrial epithelial cells, Expressed profiles, LncRNAs, mRNAs

Background

Neospora caninum, an obligate intracellular protozoan parasite similar to *Toxoplasma gondii* in morphological and biological features [1, 2], causes serious neurological disorders in canids (e.g. dogs, gray wolves and coyotes) and reproductive failure in cattle and small ruminants (e.g. goats) [3, 4]. Notably, seropositivity against *N. caninum* infection has also been reported in humans, especially in those with immunodeficiency and neurological disorders [5–7]. However, no effective drugs or vaccines against *N. caninum* infection are yet available.

In recent decades, transcriptomics has become an attractive tool for developing new diagnostic or therapeutic targets for the treatment of tumors and infectious diseases through identifying genes of interest or biological events under defined conditions or disease states [8–11]. Transcriptome analysis of bovine trophoblast cells showed a clear effect on extracellular matrix re-organization, cholesterol biosynthesis and the transcription factor AP-1 network by both Nc-Spain1H and Nc-Spain7, two *N. caninum* isolates with significantly different virulences [12]. RNA-sequencing (RNA-seq) of bovine monocyte-derived macrophages (boMØs) showed that genes involved in inflammation, chemokine signaling, cell survival and inhibition of genes related to metabolism and phagolysosome formation were upregulated. Different expression patterns of some genes encoding inflammatory cytokines (e.g. *IL12A*, *IL8* and *IL23*) were also found in boMØs infected with these two isolates [13]. Additionally, *N. caninum* infection induced significantly differentially expressed (DE) genes involved in immune response and lipid biosynthetic processes in rat brain microvascular endothelial cells (rBMVECs), human brain microvascular endothelial cells (hBMECs) [14] and mouse brain samples [15].

Long noncoding RNAs (lncRNAs), a class of RNA transcripts that are larger than 200 nucleotides (nt), exert biological functions by interacting with proteins, DNA or other RNAs at epigenetic, transcriptional and post-transcriptional levels [16, 17]. Studies have shown that dysregulation of the expression of lncRNAs occurs in a large number of diseases, including viral infections (e.g. Epstein-Barr virus, severe acute respiratory syndrome coronavirus 2 and hepatitis B virus) [18–20], bacterial infections (e.g. *Pseudomonas aeruginosa*, *Helicobacter pylori* and *Mycobacteria tuberculosis*) [21–23] and parasitic infections (e.g. *T. gondii*, *Cryptosporidium parvum* and *Eimeria necatrix*) [24–26]. These same studies and others have also shown that differentially expressed (DE) lncRNAs (DElncRNAs) were involved in several key biological processes (e.g. apoptosis, pyroptosis, cell proliferation and metabolism) [17, 27] or implicated in host–pathogen interactions (e.g. promoting or inhibiting pathogenic microorganisms) [28, 29].

The uterus is indispensable for constitution of fetal-maternal interface, embryo implantation and maintenance of pregnancy [30]. The endometrium is particularly susceptible to microbial infections, increasing the risk of adverse pregnancy outcomes [31]. *Neospora caninum* tachyzoites have been detected in the uterus of naturally infected animals, and *N. caninum* tissue cysts have also been found in the endometrium and the maternal–fetal interface (crypt) [32–34]. The objectives of the present study were to investigate the expression profiles of lncRNAs and messenger RNAs (mRNAs) in caprine endometrial epithelial cells (EECs) during *N. caninum* infection.

Methods

Parasites, cell cultures and in vitro infection model

Neospora caninum Nc-1 wild-type strain was obtained from Prof. Qun Liu (China Agricultural University, Beijing, China) and maintained in African green monkey kidney epithelial cells (Vero cells) provided as a gift by Prof. Xuefeng Qi (Northwest A&F University, Shaanxi, China). An in vitro infection model for *N. caninum* tachyzoites was established as described previously [35] by using caprine EECs supplied by Prof. Yaping Jin (Northwest A&F University, Shaanxi, China).

Sample collection

Caprine EECs in the experimental groups were infected with 1.2×10^6 freshly egressed *N. caninum* tachyzoites

at a multiplicity of infection (MOI) of 3:1 (parasite:cell) for 24 h (experimental groups: TZ1_24h to TZ3_24h) or 48 h (experimental groups: TZ1_48h to TZ3_48h). The caprine EECs without infection of tachyzoites were collected as control groups at 24 h (controls groups: C1_24h to C3_24h) or 48 h (control groups: C1_48h to C3_48h) post-infection (hpi). Cells in all experimental and control groups were collected into TRIzol (Accurate Biotechnology Co., Ltd., Hunan, China) and stored at — 80 °C until RNA extraction.

RNA extraction, library preparation and RNA-seq

Total RNA samples were extracted from each sample by using a mirVana miRNA Isolation Kit (Ambion, Austin, TX, USA) following the manufacturer's instructions. The concentration and RNA integrity of the total RNA samples were assessed using the NanoDrop spectrophotometer (Thermo Fisher Scientific, Wilmington, MA, USA) and the Agilent 2100 Bioanalyzer (Agilent Technologies, Santa Clara, CA, USA). RNA samples with a 28S:18S ratio ≥ 0.7 and RNA integrity number ≥ 7 were used for further analysis. The RNA-seq libraries were produced by using TruSeq Stranded Total RNA with Ribo-Zero Gold (Illumina Inc, San Diego, CA, USA) and sequenced using the Illumina sequencing platform (HiSeq^{TM} 2500; Illumina Inc., San Diego, CA, USA). All of these experiments were performed in the laboratory of Shanghai OE Biomedical Science and Technology Company (Shanghai, China).

Data processing and reference genome mapping

The raw reads obtained by RNA-seq were processed by using SortMeRNA software [36] to remove ribosomal RNA (rRNA) sequences, and reads with low-quality were filtered by using Trimmomatic software [37]. Fastp software [38] was then used to assess the quality of filtered reads through setting a number of important parameters, such as length distribution, Q30 and GC contents. The validated reads (clean reads) were mapped against the reference genome database (ftp://ftp.ncbi.nlm.nih.gov/genomes/all/GCF/001/704/415/GCF_001704415.1_ARS1/GCF_001704415.1_ARS1_genomic.fna.gz) using the Hisat2 (v2.2.1.0) algorithm [39].

Identification of lncRNAs

Clean reads aligned to the reference genome were assembled by using Stringtie software (v1.3.3b) [40]. The new transcripts with known coding or known loci were filtered out by comparing merged transcripts to reference transcripts. The transcripts with lengths > 200 nt and at least two exons were selected and then predicted for coding potential by using the softwares Pfam (v30) [41], coding-non-coding index (CNCI, 1.0) [42], coding potential calculator 2 (CPC2, beta) [43] and predictor of long non-coding RNAs and messenger RNAs based on an improved *k*-mer scheme (PLEK) [44] to obtain candidate lncRNAs. Known lncRNAs in these candidate lncRNAs were identified by alignment with available lncRNA databases, and unaligned candidates were referred as novel lncRNAs.

Differential expression analysis of lncRNAs and mRNAs

Expression of lncRNAs and mRNAs were analyzed by using eXpress software [45] to obtain fragments per kilobase of exon per million fragments mapped (FPKM) and count values (the number of reads between specific transcript regions). The DESEQ package (v1.18.0) was used to normalize the counts and calculate the differences in expression by comparing the *P* values and the fold change (FC). The *P* values were then adjusted by using the Benjamini and Hochberg method; genes with *q*-value or false discovery rate (FDR) < 0.05 and Log2|FC| > 1 were considered to be DE genes.

Target prediction of lncRNAs and functional analysis

The co-expression analysis between DElncRNAs (length < 6000 nt) and differentially expressed mRNAs (DEmRNAs) were conducted based on an absolute values of Pearson's correlation coefficient ≥ 0.8 and $P \leq 0.05$. Based on co-expression nets, targets for both *cis* and *trans* regulation were predicted for DElncRNAs. *Cis* targets were searched for all coding genes within 100 kb upstream or downstream of the DElncRNAs by using FEELnc software [46], while *trans* targets of DElncRNAs were screened with the number of direct complementary base pairs ≥ 10 and the base binding free energy $\leq$ - 100 by using RIsearch-2.0 software [47].

Functions of DElncRNAs were predicted through annotation of targets for both *cis* and *trans* regulation by using Gene Ontology (GO) (http://geneontology.org/) and the Kyoto Encyclopedia of Genes and Genomes (KEGG) (http://www.genome.jp/kegg/) within the Swiss-Prot database (http://www.gpmaw.com/html/swiss-prot.html) and KAAS database (http://www.genome.jp/tools/kaas/), respectively. The significance of GO terms and KEGG pathways enriched were evaluated by using the hypergeometric distribution test, with $q < 0.05$ considered to indicate significance.

Quantitative real-time PCR analysis

A total of 12 caprine EEC samples with (experimental group) or without (control group) *N. caninum* tachyzoites infection for 24 h or 48 h were collected to verify the accuracy of RNA-seq data by quantitative real-time PCR (qRT-PCR). Total RNA samples were extracted using TRIzol reagent and reversely transcribed to

complementary DNA (cDNA) by using the *EVO M-MLV* RT Kit with gDNA Clean for qPCR II (Accurate Biotechnology Co., Ltd, Hunan, China) according to the manufacturer's instructions. qRT-PCR reactions were performed by using 2 × Universal SYBR Green Fast qPCR Mix (ABclonal, Wuhan, China). The primer sequences designed using DNAMAN 7.0 software (Lynnon Biosoft, Quebec City, QC, Canada) are listed in Additional file 1: Data S1. The glyceraldehyde-3-phosphate dehydrogenase gene (*GAPDH*) was used as an internal reaction control, and three replicate assays were carried out for each gene. The relative expression of each gene was calculated by using the $2^{-\Delta\Delta Ct}$ method.

Statistical analysis

Relative expression levels of selected genes between the experimental and control groups were analyzed by using GraphPad PRISM 8.0.1 software (GraphPad Software Inc., San Diego, CA, USA), and a P value < 0.05 was considered to be statistically significant by using two-tailed t-test, with a parametric test.

Results

Identification of lncRNAs

In the present study, we generated a total of 1,306.87 M raw reads from 12 samples by using RNA-seq, of which 1280.15 M clean reads were obtained after removing the low-quality reads. The valid bases, quality score (Q30) and average GC contents of these clean reads were 95.43–96.43%, 90.40–92.82% and 48.30%, respectively (Additional file 2: Data S2). Screening using the Pfam, CNCI, CPC2 and PLEK software programs resulted in the identification of 3690 lncRNAs, including 491 novel and 3199 known lncRNAs. The total length of these lncRNAs was 6,253,838 nt and the average length was 1694.81 nt. The number of exons in most of these lncRNAs ranged from 2 to 5 (Fig. 1a, b; Additional file 3: Data S3). Four classifications were identified for these lncRNAs by both antisense and sense types: (i) genic exonic (334 antisense and 291 sense); (ii) genic intronic (395 antisense and 261 sense); (iii) intergenic downstream (291 antisense and 441 sense); and (iv) intergenic upstream (736 antisense and 331 sense) (Fig. 1c; Additional file 3: Data S3).

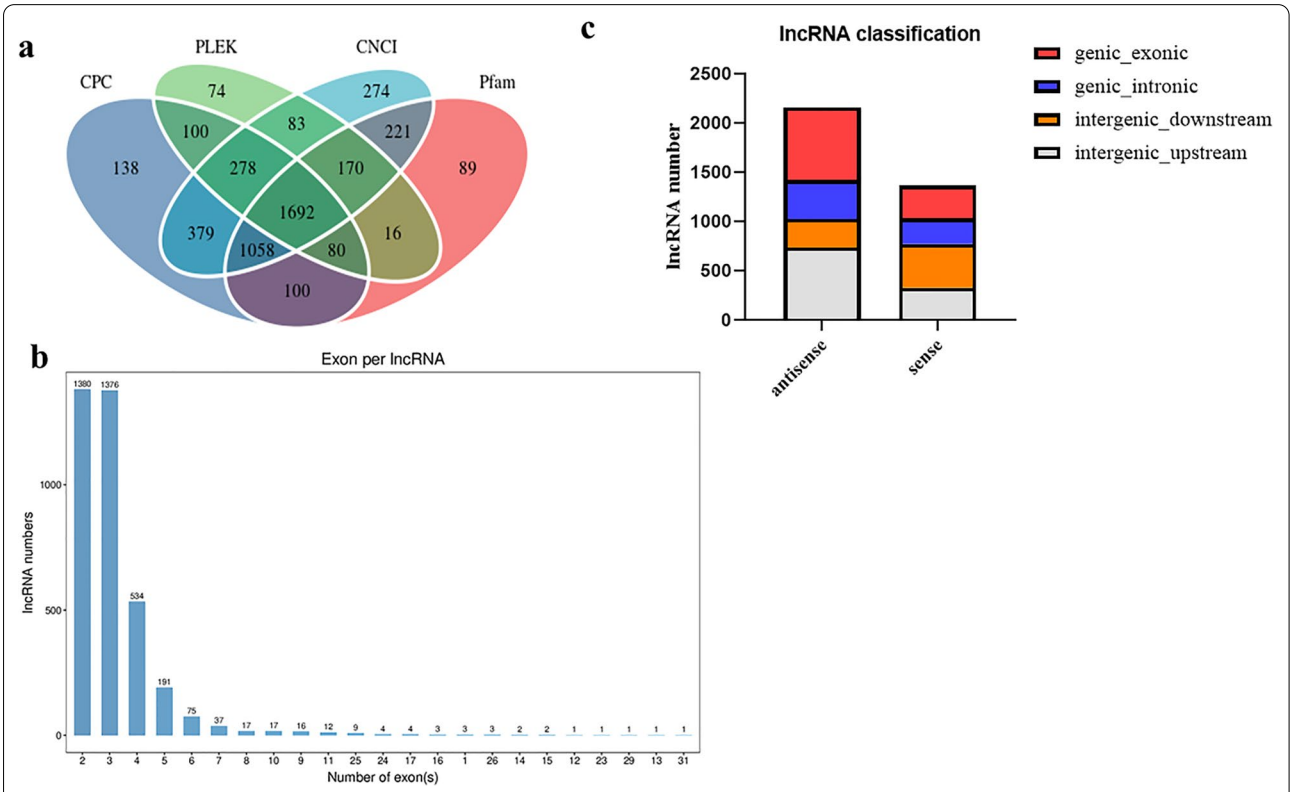

Fig. 1 Venn diagrams, exon numbers and classification of candidate long noncoding RNAs (lncRNAs) in caprine endometrial epithelial cells (EECs) following *Neospora caninum* infection. **a** Venn diagrams of coding potential analysis by using Pfam, coding-non-coding index (CNCI), coding potential calculator 2 (CPC2) and predictor of long noncoding RNAs and messenger RNAs based on an improved *k*-mer scheme (PLEK) software programs. **b** Exon numbers of lncRNAs. **c** Classification of lncRNAs by sense and antisense types

DE profiles of lncRNAs and mRNAs

To analyze DE profiles of lncRNAs and mRNAs, 12 samples were divided into three categories: (i) TZ_24 h versus C_24 h (TZ_24h-vs-C_24h); (ii) TZ_48 h versus C_48 h (TZ_48h-vs-C_48h); and (iii) TZ_48 h versus TZ_24 h (TZ_48h-vs-TZ_24h). The number of DElncRNAs in the TZ_24h-vs-C_24h, TZ_48h-vs-C_48h and TZ_48h-vs-TZ_24h categories was 88 (59 upregulated and 29 downregulated), 129 (80 upregulated and 49 downregulated) and 32 (20 upregulated and 12 downregulated), respectively (Fig. 2a; Additional file 4: Data S4). The number of DEmRNAs in the categories TZ_24h-vs-C_24h, TZ_48h-vs-C_48h and TZ_48h-vs-TZ_24h was 934 (665 upregulated and 269 downregulated), 1238 (785 upregulated and 453 downregulated) and 489 (252 upregulated and 237 downregulated), respectively (Fig. 3a; Additional file 5: Data S5). In addition, hierarchical clustering heatmaps of the DElncRNAs (length < 6000 nt) (Fig. 2b–d) and DEmRNAs (Fig. 3b–d) showed clear separation of the groups compared in each category, for all categories.

To verify the reliability of RNA-seq data, six (3 upregulated and 3 downregulated) mRNAs and nine (3 upregulated, 6 downregulated) lncRNAs were randomly selected for qRT-PCR analysis. The expression levels of *cluster of differentiation 14* (*CD14*), *mitogen-activated protein kinase kinase kinase 8* (*MAP3K8*) and *nuclear factor κB subunit 1* (*NFKB1*),

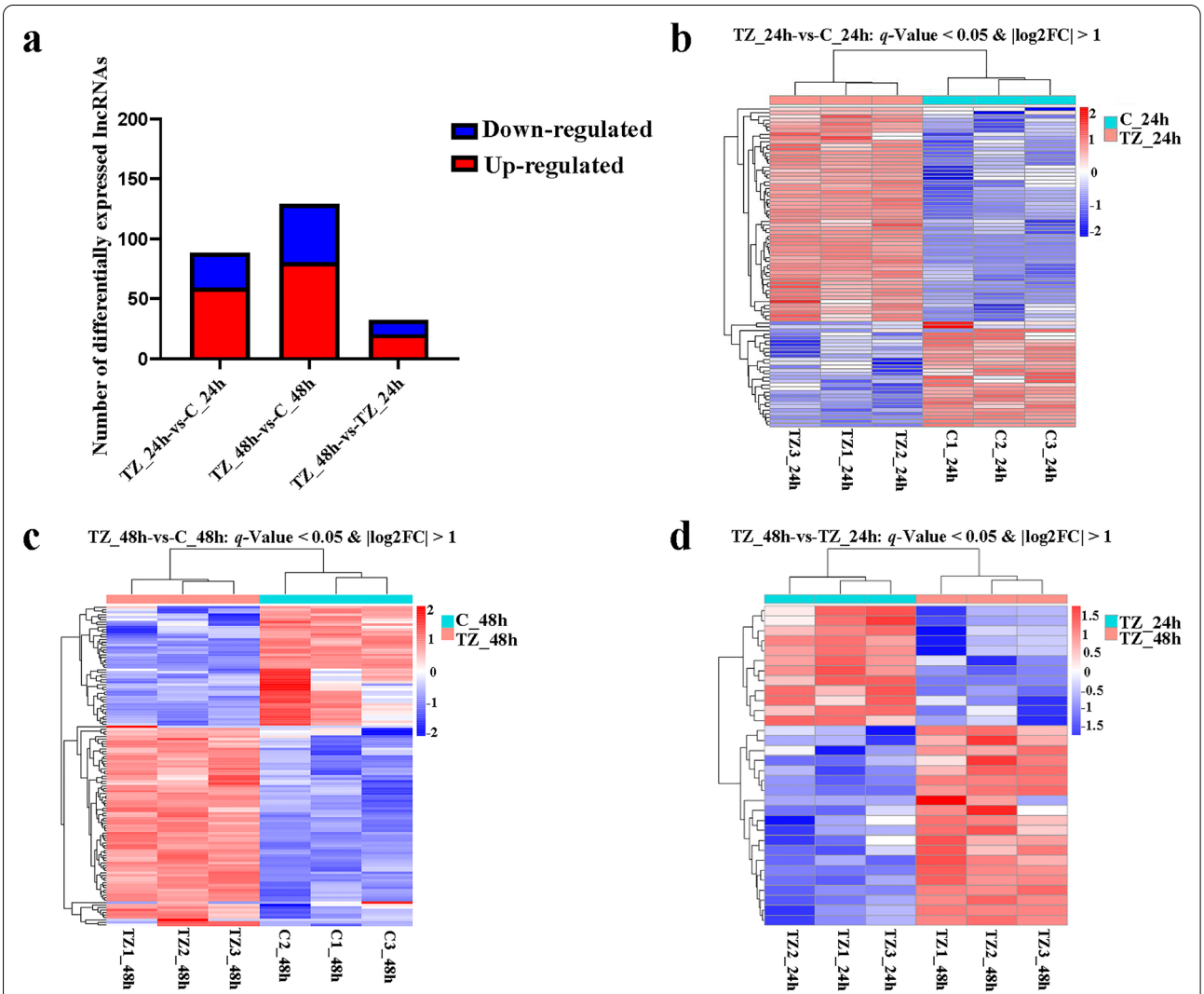

Fig. 2 Differentially expressed lncRNAs (DElncRNAs) and hierarchical clustering heatmaps of the DElncRNAs in caprine endometrial epithelial cells (EECs) following *Neospora caninum* infection. **a** The number of DElncRNAs. **b**–**d** Hierarchical clustering heatmaps of the DElncRNAs within the categories TZ_24 h versus C_24 h (TZ_24h-vs-C_24h) (**b**), TZ_48 h versus C_48 h (TZ_48h-vs-C_48h) (**c**) and TZ_48 h versus TZ_24 h (TZ_48h-vs-TZ_24h) (**d**), respectively. *P* values were adjusted by using the Benjamini and Hochberg method, with *q*-value < 0.05 and Log2|FC|> 1 considered to be significant

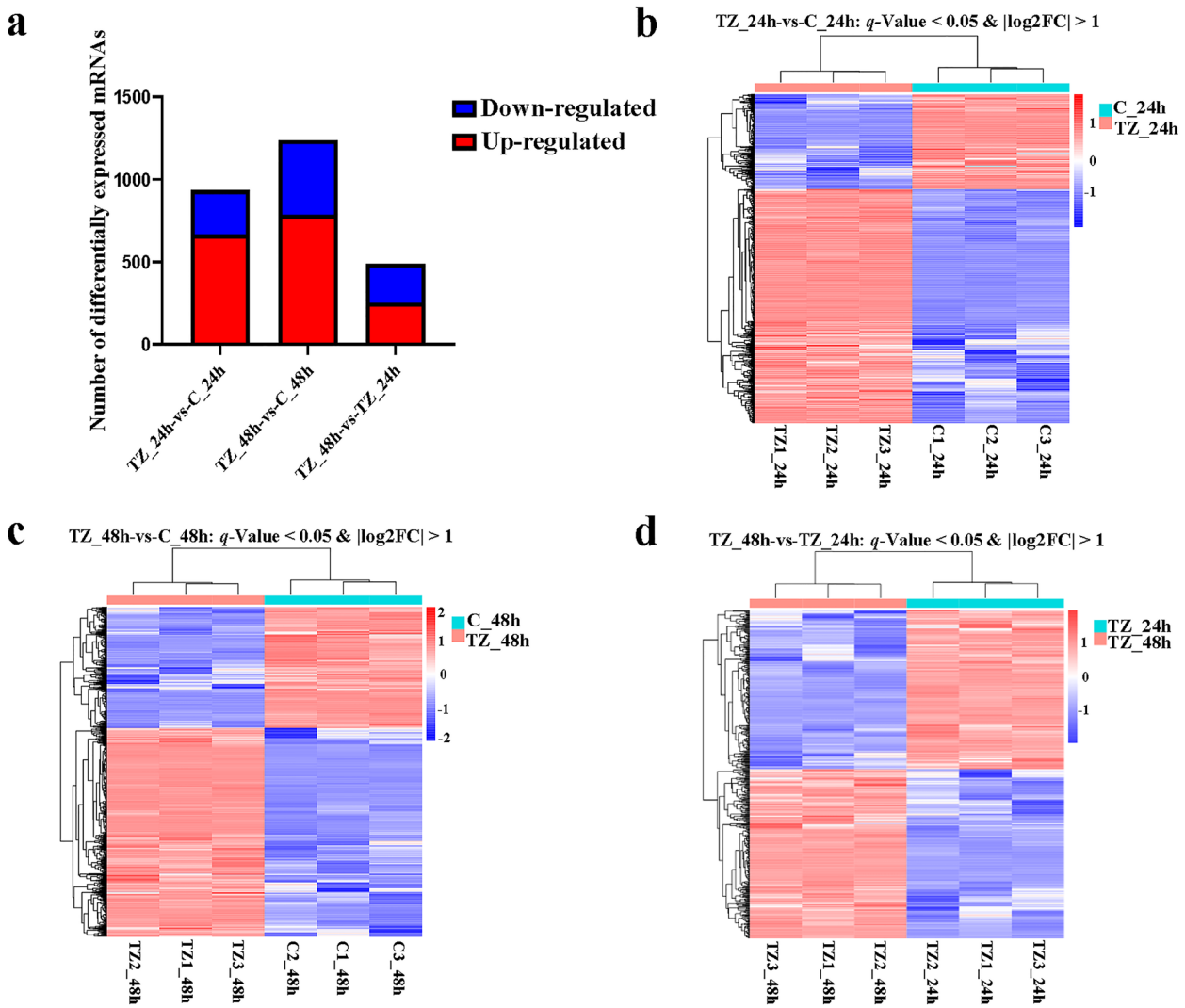

Fig. 3 Differentially expressed messenger RNAs (DEmRNAs) and hierarchical clustering heatmaps of the DEmRNAs in caprine endometrial epithelial cells (EECs) following *Neospora caninum* infection. **a** The number of DEmRNAs. **b**–**d** Hierarchical clustering heatmaps of the DEmRNAs within the categories TZ_24h-vs-C_24h (**b**), TZ_48h-vs-C_48h (**c**) and TZ_48h-vs-TZ_24h (**d**), respectively. *P* values were adjusted by using Benjamini & Hochberg method, with *q*-value < 0.05 and Log2|FC|> 1 considered to be significant

and lncRNAs *ENSCHIT00000011442*, *XR_311142.3* and *XR_001918087.1* were increased, while the expression levels of *Jun proto-oncogene* (*JUN*), *proto-oncogene c-Fos-like protein* (*FOS*) and *transforming growth factor beta 2* (*TGFB2*) and lncRNAs *ENSCHIT00000009566*, *XR_309885.2*, *XR_001295792.2*, *ENSCHIT00000002354*, *XR_001919077.1* and *ENSCHIT00000002691* were decreased in the experimental groups (Fig. 4), consistent with the transcriptome data, indicating high reproducibility and correctness of the transcriptome data by RNA-seq.

Functional prediction of the DEmRNAs

The GO enrichment analysis of DEmRNAs showed that 2590, 2971 and 1740 terms were significantly enriched within the categories TZ_24h-vs-C_24h, TZ_48h-vs-C_48h and TZ_48h-vs-TZ_24h, respectively (Additional file 6: Data S6). The top 30 most significantly enriched GO terms in cellular component (CC), biological process (BP) and molecular function (MF) are listed in Fig. 5. Of these, inflammatory response (GO: 0006954), extracellular space (GO: 0005615) and growth factor activity (GO:

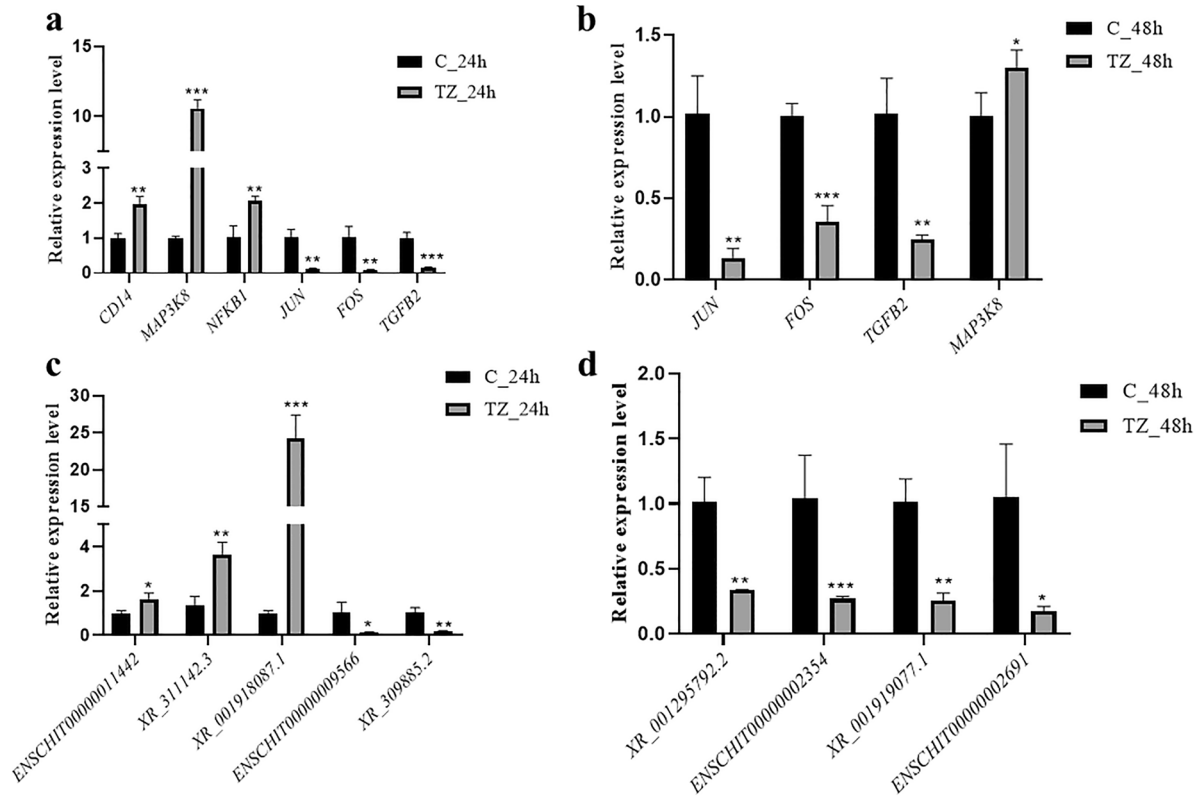

Fig. 4 Validation of the differentially expressed lncRNAs (DElncRNAs) and differentially expressed messenger RNAs (DEmRNAs) using quantitative real-time PCR (qRT-PCR). **a, b** The validation result for mRNAs in the categories TZ_24h-vs-C_24h (**a**) and TZ_48h-vs-C_48h (**b**). **c, d** The validation result for lncRNAs in the categories TZ_24h-vs-C_24h (**c**) and TZ_48h-vs-C_48h (**d**). **P* < 0.05, ***P* < 0.01, ****P* < 0.001

0008083) in the category TZ_24h-vs-C_24h, inflammatory response (GO: 0006954), nucleosome (GO: 0000786) and protein heterodimerization activity (GO: 0046982) in the category TZ_48h-vs-C_48h and nucleosome assembly (GO: 0006334), nucleosome (GO: 0000786) and protein heterodimerization activity (GO: 0046982) in the category TZ_48h-vs-TZ_24h were most significantly enriched in BP, CC and MF, respectively (Fig. 5).

KEGG pathway enrichment analysis showed that 201, 211 and 161 pathways were significantly enriched within the categories TZ_24h-vs-C_24h, TZ_48h-vs-C_48h and TZ_48h-vs-TZ_24h, respectively (Additional file 7: Data S7); the top 20 most significantly enriched pathways are listed in Fig. 6. Of these, signaling molecules and interaction (e.g. cytokine-cytokine receptor interaction, cell adhesion molecules [CAMs] and extracellular matrix [ECM]-receptor interaction), regulation of host immune response (e.g. tumor necrosis factor [TNF] signaling pathway, MAPK signaling pathway, transforming growth factor beta [TGF-beta] signaling pathway, AMPK signaling pathway, Toll-like receptor [TLR] signaling pathway and NOD-like receptor [NLR]) signaling pathway) were main pathways involved (Fig. 6). Interestingly, *N. caninum* infection induced significantly upregulated expressions of several TLR family members (e.g. *TLR2*, *TLR3* and *TLR9*), NLR family members (e.g. *NOD1* and *NLRP3*), pro-inflammatory cytokines (e.g. *IL1A*, *IL1B*, *IL6*, *IL33* and *IL34*), chemokines (e.g. *CCL20*, *CCL5*, *CXCL16*, *CXCL8* and *CX3CL1*), colony-stimulating factor (CSF) (e.g. *CSF2* and *CSF3*) and TNF receptor superfamily members (e.g. *TNFRSF21*, *TNFSF13B* and *TNFSF15*) in caprine EECs (Additional file 5: Data S5).

Co-expression analysis and prediction of DElncRNA targets

The co-expression analysis identified 61,001, 99,774 and 9306 DElncRNA-DEmRNA relationships within the categories TZ_24h-vs-C_24h, TZ_48h-vs-C_48h and TZ_48h-vs-TZ_24h, respectively (Additional file 8: Data S8). The gene co-expression networks for *cis*- and *trans*-targets of DElncRNAs are shown in Additional file 9: Fig. S1; Additional file 10: Fig. S2, respectively. Further, 30, 26 and one *cis*-targets of DElncRNAs were respectively co-expressed with 35, 29 and one DElncRNAs, comprising 35, 29 and one relationship within categories

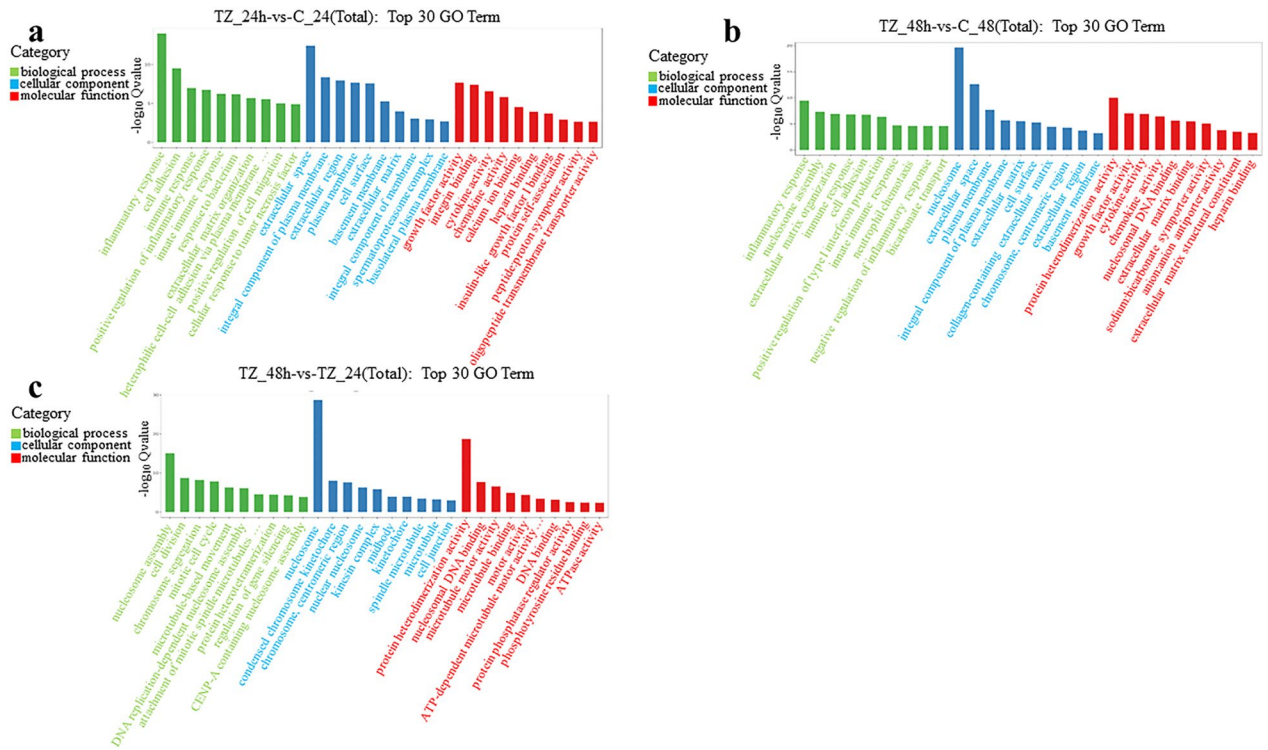

Fig. 5 Gene Ontology (GO) enrichment analysis of the differentially expressed messenger RNAs (DEmRNAs) in caprine endometrial epithelial cells (EECs) following *Neospora caninum* infection. **a-c** The top 30 GO terms enriched with DEmRNAs within the categories TZ_24h-vs-C_24h (**a**), TZ_48h-vs-C_48h (**b**) and TZ_48h-vs-TZ_24h (**c**), respectively. A *q*-value < 0.05 and Log2|FC|> 1 were considered to be significant

TZ_24h-vs-C_24h, TZ_48h-vs-C_48h and TZ_48h-vs-TZ_24h, respectively (Additional file 11: Data S9). 83, 130 and 30 *trans*-targets of DElncRNAs were respectively predicted for 28, 41 and 10 DElncRNAs, comprising 460, 957 and 110 relationships within categories TZ_24h-vs-C_24h, TZ_48h-vs-C_48h and TZ_48h-vs-TZ_24h, respectively (Additional file 12: Data S10).

Functional analysis of the targets for DElncRNAs

The GO enrichment analyses of potential *cis*-targets of DElncRNAs showed that 254, 232 and 44 terms were significantly enriched in the categories TZ_24h-vs-C_24h, TZ_48h-vs-C_48h and TZ_48h-vs-TZ_24h, respectively (Additional file 13: Data S11). Further, 534, 701 and 1694 terms of potential *trans*-targets of DElncRNAs were found to be significantly enriched in the categories TZ_24h-vs-C_24h, TZ_48h-vs-C_48h and TZ_48h-vs-TZ_24h, respectively (Additional file 14: Data S12). The top 30 most significantly enriched GO terms of potential *cis*-targets and *trans*-targets of DElncRNAs in BP, CC and MF are listed in Fig. 7 and Additional file 15: Fig. S3.

KEGG pathway enrichment analysis of potential *cis*-targets of DElncRNAs showed that 55, 47 and 20 pathways were significantly enriched within the categories TZ_24h-vs-C_24h, TZ_48h-vs-C_48h and TZ_48h-vs-TZ_24h, respectively (Additional file 16: Data S13) and that 62, 80 and 158 pathways of potential *trans*-targets of DElncRNAs were significantly enriched within the categories TZ_24h-vs-C_24h, TZ_48h-vs-C_48h and TZ_48h-vs-TZ_24h, respectively (Additional file 17: Data S14). The top 20 most significantly enriched pathways are listed in Fig. 8 and Additional file 18: Fig. S4. Of these, signal transduction (e.g. MAPK signaling pathway, PPAR signaling pathway, ErbB signaling pathway, calcium signaling pathway, TNF signaling pathway and AMPK signaling pathway), neural transmission (e.g. GABAergic synapse, serotonergic synapse, cholinergic synapse, glutamatergic synapse, dopaminergic synapse, retrograde endocannabinoid signaling), signaling molecules and interaction (e.g. cytokine-cytokine receptor interaction, ECM-receptor interaction and CAMs), and metabolism (e.g. glycosphingolipid biosynthesis-lacto and neolacto series, glycosaminoglycan biosynthesis-heparan sulfate/heparin, 2-Oxocarboxylic acid, propanoate, beta-alanine, tryptophan, vitamin B6, primary bile acid biosynthesis) were main pathways involved in.

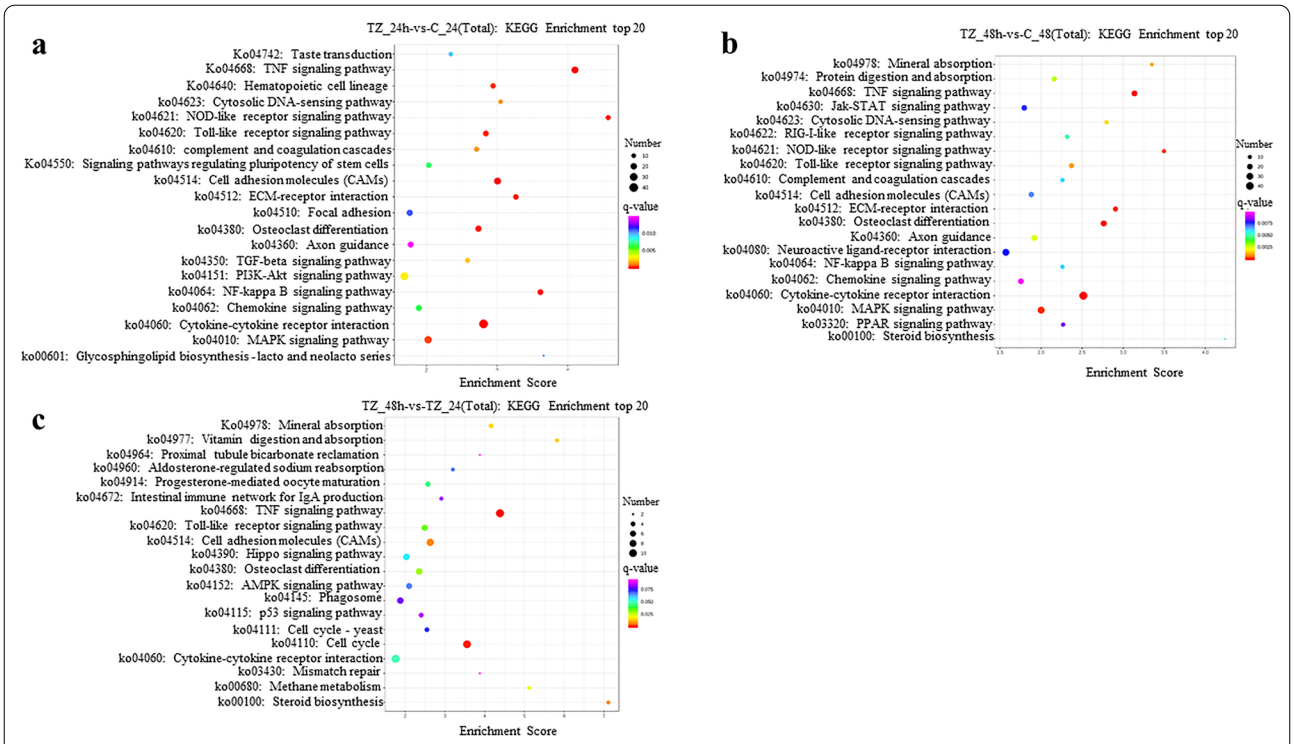

Fig. 6 Kyoto Encyclopedia of Genes and Genomes (KEGG) pathway enrichment analysis of the differentially expressed messenger RNAs (DEmRNAs) in caprine endometrial epithelial cells (EECs) following *Neospora caninum* infection. **a**–**c** The top 20 KEGG pathway terms enriched with DEmRNAs within the categories TZ_24h-vs-C_24h (**a**), TZ_48h-vs-C_48h (**b**) and TZ_48h-vs-TZ_24h (**c**), respectively. A *q*-value < 0.05 and Log2|FC|> 1 were considered to be significant

Discussion

The uterus, one of the main reproductive organs needed to maintain normal pregnancy, can be naturally infected by *N. caninum* [32–34]. Previous studies mainly focused on bio-functions of host protein-coding genes [48, 49] or on organelles of *N. caninum* tachyzoites (e.g. microneme, rhoptry and dense granule) [50–52] during *N. caninum* infection, but the role of host lncRNAs during *N. caninum* infection has not been investigated prior to the present study. Recent studies have shown that host lncRNAs play important roles in cellular molecular regulatory networks, and these have been reported to be closely related to the pathogenesis of apicomplexan parasites [53]. For example, genome-wide RNA transcriptome analysis identified 3942 DEmRNAs and 1839 DElncRNAs in murine intestinal epithelial cells following *Cryptosporidium parvum* infection. Of these, a lncRNA, named *NR_045064*, could reduce infection burden of parasites in murine intestinal epithelial cells in vitro and in the enteroids of neonatal mice by promoting expression of host defense genes (e.g. *Csf2*, *Nos2*, and *Cxcl2*) [54]. Similarly, a total of 109 DEmRNAs and 996 DElncRNAs were identified in human foreskin fibroblast (HFF) cells infected with *Toxoplasma gondii* by using microarray, and a novel lncRNA, named *NONSHAT022487* was found to be able to decrease the expression of several host cytokines (e.g. *IFN-γ*, *TNF-α*, *IL-1β* and *IL-12*) by negatively regulating the immune-related molecule *UNC93B1* [55]. In the present study, we found that *N. caninum* infection significantly altered the expression of mRNAs and lncRNAs in caprine EECs at 24 and 48 hpi.

Pattern recognition receptors (PRRs) are pivotal parts of host innate immunity that recognize specific pathogen-associated molecular patterns (PAMPs) to induce secretion of inflammatory cytokines and chemokines through initiating intracellular signaling cascades, ultimately eliminating invading pathogens and infected cells [56]. These PRRs include TLRs, NLRs, RIG-I-like receptors (RLRs) and C-type lectin receptors (CLRs). Among them, TLRs and NLRs play important roles in mediating host innate and adaptive immune responses against *N. caninum* infection [48, 57, 58]. The expression of *TLR2* was efficiently activated in immune cells (e.g. bovine/mouse peritoneal macrophage cell) infected with *N. caninum* or treated with its derived antigens (e.g. glycosylphosphatidylinositol [GPI], extracellular vesicles [EVs], soluble antigens, *N. caninum* cyclophilin [NcCyp]) and could remarkably enhance production of Th1 immune

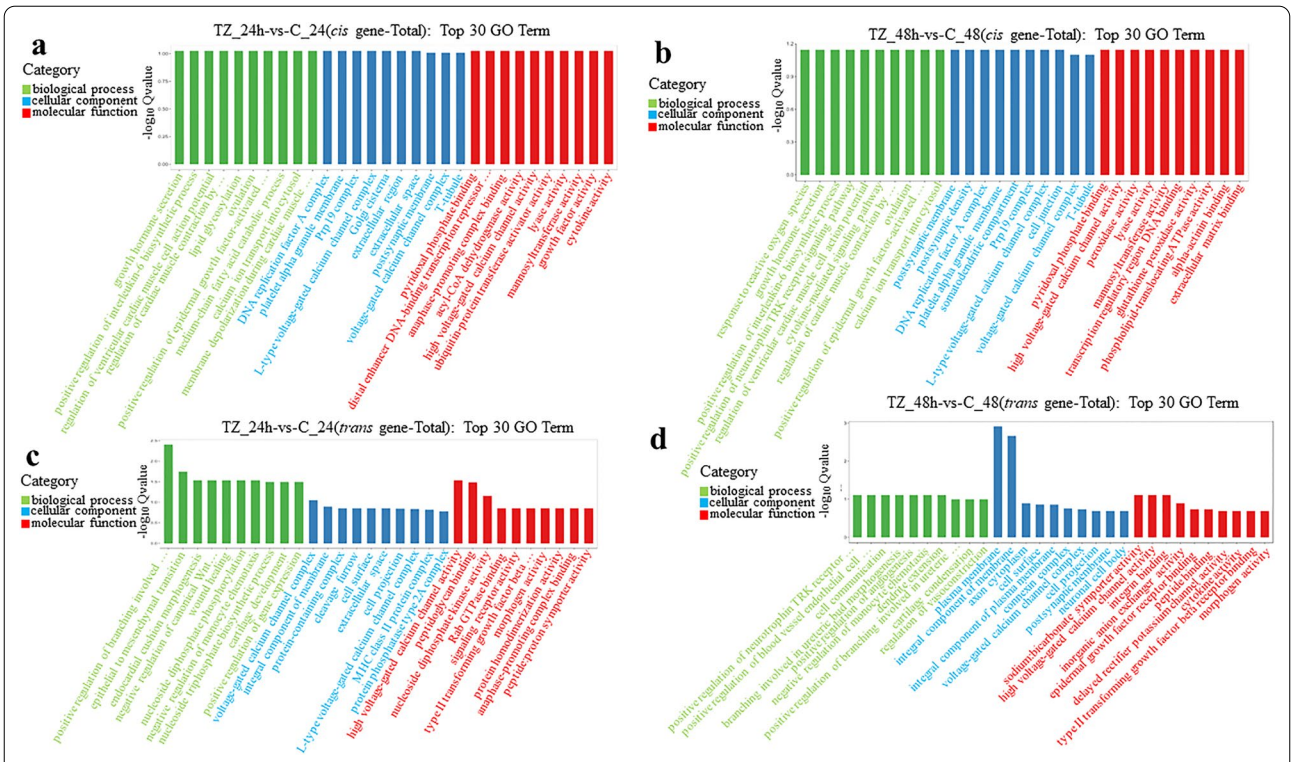

Fig. 7 Gene Ontology (GO) enrichment analysis for the *cis*- and *trans*-targets of the differentially expressed lncRNAs (DElncRNAs) in caprine endometrial epithelial cells (EECs) following *Neospora caninum* infection. **a**–**d** The top 30 GO terms enriched for the *cis*- (**a, b**) and *trans*- (**c, d**) targets of DElncRNAs within the categories TZ_24h-vs-C_24h and TZ_48h-vs-C_48h, respectively. A *q*-value < 0.05 and Log2|FC|> 1 were considered to be significant

responses, which is critical for controlling *N. caninum* infection. *TLR2* knockout (*TLR2*$^{-/-}$) mice displayed higher parasite loads than wild-type mice [58–62]. *TLR3* was also activated in murine macrophages infected with *N. caninum*, and it could enhance expression of the type I interferon (*IFN-α* and *IFN-β*) by initiating adaptor protein TRIF. *TLR3* knockout (*TLR3*$^{-/-}$) mice reduced the survival rates of infected mice [57]. Furthermore, in non-professional immune cells, the expression of *TLR2* was also induced in both bovine trophoblast cells and caruncular cells infected with *N. caninum* [63], and *TLR3*, *7*, *8* and *9* were upregulated in the maternal–fetal interface in cattle infected with *N. caninum* or immunized with soluble whole antigens or recombinant *N. caninum* proteins [64, 65]. In our study, *TLR2*, *TLR3* and *TLR9* were significantly upregulated in caprine EECs infected with *N. caninum*, consistent with gene expression profiling in boMØs infected with *N. caninum* [13]. In addition, *NLRP3* inflammasome and *NOD1* were also activated in caprine EECs infected with *N. caninum*. Previous studies showed that *N. caninum* infection activated the *NLRP3* inflammasome in murine bone marrow-derived macrophages or bovine peritoneal macrophage cells, accompanied by cleavage of *caspase-1*, release of *IL-1β* and *IL-18*, as well as cell death against *N. caninum* infection, and *NLRP3* knockout (*NLRP3*$^{-/-}$) mice displayed a high susceptibility to *N. caninum* infection [66, 67]. Although the role of *NOD1* in host cells infected with *N. caninum* remains unknown, *NOD1* can mediate host defenses against bacterial, viral and other parasitic infections [68]. These findings suggest that activation of TLRs and NLRs in caprine EECs during *N. caninum* would trigger protective innate defense mechanisms against *N. caninum* infection.

Cytokines are major messenger proteins of inflammatory process and immune responses with various biological effects (e.g. cell growth, differentiation, inflammatory response and immune defense) [69]. Previous studies have confirmed that pro-inflammatory cytokines (e.g. *IFN-γ*, *TNF-α*, *IL-12*, *IL6* and *IL1β*) induced by *N. caninum* infection could exert protective immunity to inhibit the multiplication of *N. caninum* both in vitro [70, 71] and in vivo [59, 72]. In our study, a large number of pro-inflammatory cytokines (e.g. *IL1A*, *IL1B*, *IL6*, *IL33* and *IL34*) were up-regulated, and the anti-inflammatory cytokines (e.g. *TGFB2* and *TGFB3*) was down-regulated, suggesting that *N. caninum* infection

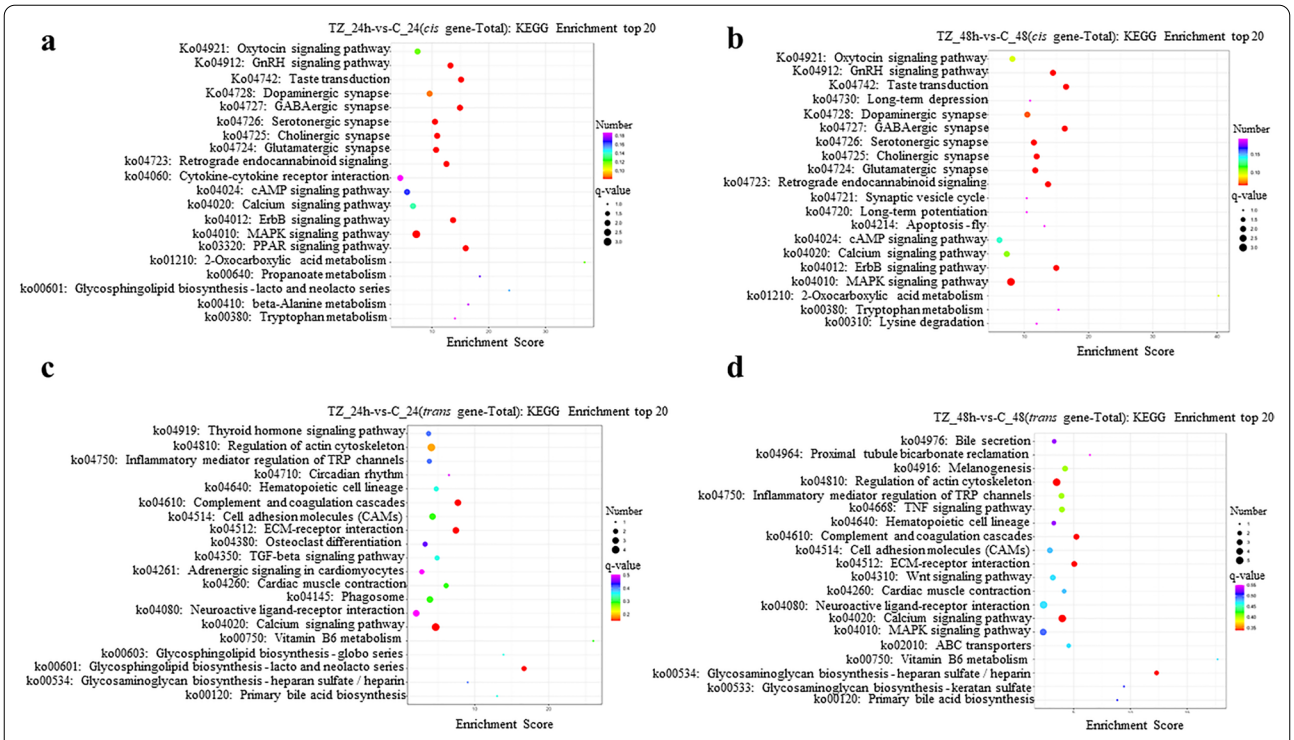

Fig. 8 Kyoto Encyclopedia of Genes and Genomes (KEGG) pathway enrichment analysis for the *cis*- and *trans*-targets of the differentially expressed lncRNAs (DElncRNAs) in caprine endometrial epithelial cells (EECs) following *Neospora caninum* infection. **a**–**d** The top 20 KEGG pathway terms enriched for the *cis*- (**a, b**) and *trans*- (**c, d**) targets of DElncRNAs within the categories TZ_24h-vs-C_24h and TZ_48h-vs-C_48h, respectively. *q*-value < 0.05 and Log2|FC| > 1 are considered to be significant

promoted the secretion of pro-inflammatory cytokines in caprine EECs. In addition, chemokines (e.g. *CCL20*, *CCL5*, CXCL16, *CXCL8* and *CX3CL1*), colony-stimulating factor (e.g. *CSF2* and *CSF3*) and tumor necrosis factor receptor superfamily member (e.g. *TNFRSF21*, *TNFSF13B* and *TNFSF15*) involved in immune modulatory properties were also upregulated in caprine EECs during *N. caninum* infection. These data suggest that cytokines induced by *N. caninum* infection in caprine EECs would be a strategy for eliciting immune responses at the maternal–fetal interface against *N. caninum* infection, but the disruption of the immune balance at the maternal–fetal interface was also reported to lead to miscarriage [73, 74].

To understand the potential regulatory functions of DElncRNAs in caprine EECs during *N. caninum* infection, we predicted the *cis*- and *trans*-targets of DElncRNAs by constructing lncRNA-mRNA co-expression networks. We found that numerous biological signal pathways were significantly enriched, including MAPK signaling pathway, PPAR signaling pathway, ErbB signaling pathway, calcium signaling pathway, TNF signaling pathway and AMPK signaling pathway. These pathways have been reported to be involved in the regulation of important biological processes, such as cell proliferation, apoptosis, autophagy, inflammatory and immune response [75–80]. For example, upregulated expressions of lncRNA *XR_001296952.2* and lncRNA *XR_001919803.1* were found to *cis*-regulate the expression of *stanniocalcin-2* (*STC2*), which could promote proliferation and inhibit apoptosis in caprine EECs through the RAS/RAF/MEK/ERK signaling pathways [81], and could also enhance autophagy through the PI3K/AKT/AMPK signaling pathways [82]. Previous studies have reported that activation of autophagy facilitated the proliferation of *N. caninum* both in vitro [35] and in vivo [83]. In bone marrow-derived macrophages, the activation of p38 MAPK was found to be associated with immune evasion of *N. caninum* [84]. However, in Madin-Darby bovine kidney (MDBK) cells, p38 MAPK inhibitor effectively inhibited *N. caninum* tachyzoite motility and micronemal protein secretion and reduced cell invasion of *N. caninum* [85]. In addition, neural transmission (e.g. GABAergic synapse, serotonergic synapse, cholinergic synapse, glutamatergic synapse, dopaminergic synapse and retrograde endocannabinoid signaling), metabolism processes (e.g. glycosphingolipid biosynthesis-lacto and neolacto series, glycosaminoglycan biosynthesis-heparan sulfate/heparin, 2-oxocarboxylic acid, propanoate, beta-alanine, tryptophan,

vitamin B6 and primary bile acid biosynthesis) and signaling molecules and interaction (e.g. cytokine-cytokine receptor interaction, ECM-receptor interaction and CAMs) were also significantly enriched for DElncRNA targets, indicating that these DElncRNAs would play roles in regulating host neural transmission, metabolism processes and interactions between signaling molecules during *N. caninum* infection. Both ECM-receptor interaction and CAMs are associated with endometrial receptivity, the key to successful implantation and development of mammalian embryos [86, 87], suggesting that these lncRNA targets would influence the outcome of pregnancy during *N. caninum* infection.

Conclusions

Neospora caninum infection significantly altered the expression profiles of mRNAs and lncRNAs in caprine EECs at 24 and 48 hpi. The identified DEmRNAs and DElncRNAs were involved in immune response, signal transduction, nervous and metabolic processes during *N. caninum* infection. To our knowledge, this is the first investigation of global profiles of host lncRNAs during *N. caninum* infection. The results provide novel insight into understanding the underlying pathogenesis of *N. caninum* in maternal–fetal interface. However, since functions of most goat lncRNAs identified in our study are still unknown, computerized prediction of their function is very difficult if not completely impossible. Therefore, further studies should be conducted to reveal the mysterious veil of these identified DElncRNAs in future studies.

Abbreviations

boMØs: Bovine monocyte-derived macrophages; BP: Biological process; CAMs: Cell adhesion molecules; CC: Cellular component; CNCI: Coding-noncoding index; CPC2: Coding potential calculator 2; DE: Differentially expressed; DElncRNAs: Differentially expressed lncRNAs; DEmRNAs: Differentially expressed mRNAs; EECs: Endometrial epithelial cells; FC: Fold change; GO: Gene Ontology; hpi: Hours post-infection; KEGG: Kyoto Encyclopedia of Genes and Genomes; lncRNAs: Long noncoding RNAs; MF: Molecular function; NLR: NOD-like receptor; mRNAs: Messenger RNAs; PLEK: Predictor of long-noncoding RNAs and messenger RNAs based on an improved *k*-mer scheme; PRRs: Pattern recognition receptors; qRT-PCR: Quantitative real-time PCR; RNA-seq: RNA sequencing; *TGFB2*: *Transforming growth factor beta 2*; TLRs: Toll-like receptors; *TNF*: *Tumor necrosis factor*.

Supplementary Information

The online version contains supplementary material available at https://doi.org/10.1186/s13071-022-05405-5.

Additional file 1: Data S1. The primer sequences used in this study by quantitative real-time PCR (qRT-PCR).

Additional file 2: Data S2. The statistics of sequencing data.

Additional file 3: Data S3. Length, exon numbers and classification of the long noncoding RNAs (lncRNAs).

Additional file 4: Data S4. All differentially expressed lncRNAs (DElncRNAs).

Additional file 5: Data S5. All differentially expressed mRNAs (DEmRNAs).

Additional file 6: Data S6. Gene Ontology (GO) enrichment analysis of all differentially expressed mRNAs (DEmRNAs).

Additional file 7: Data S7. Kyoto Encyclopedia of Genes and Genomes (KEGG) pathway analysis of all differentially expressed mRNAs (DEmRNAs).

Additional file 8: Data S8. The gene co-expression analysis of differentially expressed (DE) lncRNAs and DEmRNAs.

Additional file 9: Figure S1. The gene co-expression networks of *cis*-targets of differentially expressed lncRNAs (DElncRNAs) in caprine endometrial epithelial cells (EECs) following *Neospora caninum* infection. **a**-**c** The top 20 most significantly enriched *cis*-targets of DElncRNAs within the categories TZ_24h-vs-C_24h (**a**), TZ_48h-vs-C_48h (**b**), and TZ_48h-vs-TZ_24h (**c**), respectively. The left and right sides of the *y*-axis represent mRNA and lncRNA, respectively, and the *x*-axis represents the distance between mRNA and lncRNA, with negative values representing upstream and positive values representing downstream. **P*< 0.05, ***P*< 0.01, ****P*< 0.001.

Additional file 10: Figure S2. The gene co-expression networks of *trans*-targets of differentially expressed lncRNAs (DElncRNAs) in caprine endometrial epithelial cells (EECs) following *Neospora caninum* infection. **a**-**c** Co-repression network of DElncRNAs with their *trans*-targets within the categories TZ_24h-vs-C_24h (**a**), TZ_48h-vs-C_48h (**b**), and TZ_48h-vs-TZ_24h (**c**), respectively. The red nodes represent lncRNAs, the green nodes represent mRNAs, and the node size represents the number of genes.

Additional file 11: Data S9. The *cis*-target genes predicted for differentially expressed lncRNAs (DElncRNAs).

Additional file 12: Data S10. The *trans*-target genes predicted for differentially expressed lncRNAs (DElncRNAs).

Additional file 13: Data S11. Gene Ontology (GO) enrichment analysis of all *cis*-target genes for the differentially expressed lncRNAs (DElncRNAs).

Additional file 14: Data S12. Gene Ontology (GO) enrichment analysis of all *trans*-target genes for the differentially expressed lncRNAs (DElncRNAs).

Additional file 15: Figure S3. Gene Ontology (GO) enrichment analysis for the *cis*- and *trans*-targets of the differentially expressed lncRNAs (DElncRNAs) in caprine endometrial epithelial cells (EECs) following *Neospora caninum* infection. **a**, **b** The top 30 GO terms enriched for the *cis*- (**a**) and *trans*- (**b**) targets of DElncRNAs within the category TZ_48h-vs-TZ_24h. A *q*-value < 0.05 and Log2|FC| > 1 are considered to be significant.

Additional file 16: Data S13. Kyoto Encyclopedia of Genes and Genomes (KEGG) pathway enrichment analysis of all *cis*-target genes for the differentially expressed lncRNAs (DElncRNAs).

Additional file 17: Data S14. Kyoto Encyclopedia of Genes and Genomes (KEGG) pathway enrichment analysis of all *trans*-target genes for the differentially expressed lncRNAs (DElncRNAs).

Additional file 18: Figure S4. Kyoto Encyclopedia of Genes and Genomes (KEGG) pathway enrichment analysis for the *cis*- and *trans*-targets of the differentially expressed lncRNAs (DElncRNAs) in caprine endometrial epithelial cells (EECs) following *Neospora caninum* infection., The top 20 KEGG pathway terms enriched for the *cis*- (a) and *trans*- (b) targets of DElncRNAs within the category TZ_48h-vs-TZ_24h. A *q*-value < 0.05 and Log2|FC| > 1 are considered to be significant.

Acknowledgements
The authors are grateful to Professors Yaping Jin and Xuefeng Qi from Northwest A&F University for providing the passage cells, and to Professor Qun Liu from China Agricultural University for kindly providing the *N. caninum* Nc-1 wild-type strain.

Author contributions
GHZ and XQZ designed the experiments and critically revised the manuscript. SSZ, and DLT performed the experiments, with the help from JMC, JPW, XY and JKS for analyzing the data. SSZ and GHZ wrote the manuscript, with active inputs from XY and JKS. All authors read and approved the final manuscript.

Funding
This work was supported by grants from the Innovation Support Plan of Shaanxi Province (Grant No. 2021TD-31), the Key Research and Development Program of Shaanxi Province (Grant No. 2022NY-097), the Fund for Shanxi "1331 Project" (Grant No. 20211331-13), the Special Research Fund of Shanxi Agricultural University for High-level Talents (Grant No. 2021XG001) and Yunnan Expert Workstation (Grant No. 202005AF150041).

Availability of data and materials
The datasets supporting the findings of this article are included within the article and its additional files. The original data were deposited in the NCBI repository under accession number is PRJNA838937.

Declarations

Ethics approval and consent to participate
Not applicable.

Consent for publication
Not applicable.

Competing interests
The authors declare that they have no competing interests. The co-corresponding author, Professor Xing-Quan Zhu, serves as the Subject Editor for the section "Parasite genetics, genomics and proteomics" of ***Parasites & Vectors***.

Author details
[1]College of Veterinary Medicine, Northwest A&F University, Yangling 712100, Shaanxi, China. [2]College of Veterinary Medicine, Shanxi Agricultural University, Taigu 030801, Shanxi, China. [3]Key Laboratory of Veterinary Public Health of Higher Education of Yunnan Province, College of Veterinary Medicine, Yunnan Agricultural University, Kunming 650201, Yunnan, China.

Received: 8 June 2022 Accepted: 19 July 2022
Published online: 24 August 2022

References

1. Speer CA, Dubey JP, McAllister MM, Blixt JA. Comparative ultrastructure of tachyzoites, bradyzoites, and tissue cysts of *Neospora caninum* and *Toxoplasma gondii*. Int J Parasitol. 1999;29:1509–19.
2. Reid AJ, Vermont SJ, Cotton JA, Harris D, Hill-Cawthorne GA, Könen-Waisman S, et al. Comparative genomics of the apicomplexan parasites *Toxoplasma gondii* and *Neospora caninum*: Coccidia differing in host range and transmission strategy. PLoS Pathog. 2012;8:e1002567.
3. Dubey JP, Schares G. Neosporosis in animals-the last five years. Vet Parasitol. 2011;180:90–108.
4. Sánchez-Sánchez R, Vázquez P, Ferre I, Ortega-Mora LM. Treatment of toxoplasmosis and neosporosis in farm ruminants: state of knowledge and future trends. Curr Top Med Chem. 2018;18:1304–23.
5. Tranas J, Heinzen RA, Weiss LM, McAllister MM. Serological evidence of human infection with the protozoan *Neospora caninum*. Clin Diagn Lab Immunol. 1999;6:765–7.
6. Oshiro LM, Motta-Castro AR, Freitas SZ, Cunha RC, Dittrich RL, Meirelles AC, et al. *Neospora caninum* and *Toxoplasma gondii* serodiagnosis in human immunodeficiency virus carriers. Rev Soc Bras Med Trop. 2015;48:568–72.
7. Lobato J, Silva DA, Mineo TW, Amaral JD, Segundo GR, Costa-Cruz JM, et al. Detection of immunoglobulin G antibodies to *Neospora caninum* in humans: high seropositivity rates in patients who are infected by human immunodeficiency virus or have neurological disorders. Clin Vaccine Immunol. 2006;13:84–9.
8. Qin L, Huang D, Huang J, Huang H. New biomarkers and therapeutic targets of human liver cancer: transcriptomic findings. BioFactors. 2021;47:1016–31.
9. Banchereau R, Cepika AM, Banchereau J, Pascual V. Understanding human autoimmunity and autoinflammation through transcriptomics. Annu Rev Immunol. 2017;35:337–70.
10. Dey-Rao R, Sinha AA. Vitiligo blood transcriptomics provides new insights into disease mechanisms and identifies potential novel therapeutic targets. BMC Genomics. 2017;18:109.
11. Le BL, Andreoletti G, Oskotsky T, Vallejo-Gracia A, Rosales R, Yu K, et al. Transcriptomics-based drug repositioning pipeline identifies therapeutic candidates for COVID-19. Sci Rep. 2021;11:12310.
12. Horcajo P, Jiménez-Pelayo L, García-Sánchez M, Regidor-Cerrillo J, Collantes-Fernández E, Rozas D, et al. Transcriptome modulation of bovine trophoblast cells in vitro by *Neospora caninum*. Int J Parasitol. 2017;47:791–9.
13. García-Sánchez M, Jiménez-Pelayo L, Horcajo P, Collantes-Fernández E, Ortega-Mora LM, Regidor-Cerrillo J. *Neospora caninum* infection induces an isolate virulence-dependent pro-inflammatory gene expression profile in bovine monocyte-derived macrophages. Parasit Vectors. 2020;13:374.
14. Elsheikha HM, Alkurashi M, Palfreman S, Castellanos M, Kong K, Ning E, et al. Impact of *Neospora caninum* infection on the bioenergetics and transcriptome of cerebrovascular endothelial cells. Pathogens. 2020;9:710.
15. Nishimura M, Tanaka S, Ihara F, Muroi Y, Yamagishi J, Furuoka H, et al. Transcriptome and histopathological changes in mouse brain infected with *Neospora caninum*. Sci Rep. 2015;5:7936.
16. Dykes IM, Emanueli C. Transcriptional and post-transcriptional gene regulation by long non-coding RNA. Genom Proteom Bioinform. 2017;15:177–86.
17. Chi Y, Wang D, Wang J, Yu W, Yang J. Long non-coding RNA in the pathogenesis of cancers. Cells. 2019;8:1015.
18. Wang C, Li D, Zhang L, Jiang S, Liang J, Narita Y, et al. RNA sequencing analyses of gene expression during Epstein-Barr virus infection of primary B lymphocytes. J Virol. 2019;93:e00226-19.
19. Feng J, Yang G, Liu Y, Gao Y, Zhao M, Bu Y, et al. LncRNA PCNAP1 modulates hepatitis B virus replication and enhances tumor growth of liver cancer. Theranostics. 2019;9:5227–5245.
20. Vishnubalaji R, Shaath H, Alajez NM. Protein coding and long noncoding RNA (lncRNA) transcriptional landscape in SARS-CoV-2 infected bronchial epithelial cells highlight a role for interferon and inflammatory response. Genes (Basel). 2020;11:760.
21. Balloy V, Koshy R, Perra L, Corvol H, Chignard M, Guillot L, et al. Bronchial epithelial cells from cystic fibrosis patients express a specific long non-coding RNA signature upon *Pseudomonas aeruginosa* infection. Front Cell Infect Microbiol. 2017;7:218.
22. Yousefi L, Osquee HO, Ghotaslou R, Rezaee MA, Pirzadeh T, Sadeghi J, et al. Dysregulation of lncRNA in *Helicobacter pylori*-infected gastric cancer cells. Biomed Res Int. 2021;2021:6911734.
23. Huang Z, Liu J, Li L, Guo Y, Luo Q, Li J. Long non-coding RNA expression profiling of macrophage line RAW264.7 infected by Mycobacterium tuberculosis. Biotech Histochem. 2020;95:403–10.
24. Wang SS, Zhou CX, Elsheikha HM, He JJ, Zou FC, Zheng WB, et al. Temporal transcriptomic changes in long non-coding RNAs and messenger RNAs involved in the host immune and metabolic response during *Toxoplasma gondii* lytic cycle. Parasit Vectors. 2022;15:22.
25. Liu TL, Fan XC, Li YH, Yuan YJ, Yin YL, Wang XT, et al. Expression profiles of mRNA and lncRNA in HCT-8 cells infected with *Cryptosporidium parvum* IId subtype. Front Microbiol. 2018;9:1409.
26. Fan XC, Liu TL, Wang Y, Wu XM, Wang YX, Lai P, et al. Genome-wide analysis of differentially expressed profiles of mRNAs, lncRNAs and circRNAs in chickens during *Eimeria necatrix* infection. Parasit Vectors. 2020;13:167.
27. Liu J, Yao L, Zhang M, Jiang J, Yang M, Wang Y. Downregulation of LncRNA-XIST inhibited development of non-small cell lung cancer by activating miR-335/SOD2/ROS signal pathway mediated pyroptotic cell death. Aging (Albany NY). 2019;11:7830–46.
28. Wen Y, Chen H, Luo F, Zhou H, Li Z. Roles of long noncoding RNAs in bacterial infection. Life Sci. 2020;263:118579.

29. Fortes P, Morris KV. Long noncoding RNAs in viral infections. Virus Res. 2016;212:1–11.
30. Yang S, Wang H, Li D, Li M. Role of endometrial autophagy in physiological and pathophysiological processes. J Cancer. 2019;10:3459–71.
31. Turner ML, Healey GD, Sheldon IM. Immunity and inflammation in the uterus. Reprod Domest Anim. 2012;47:402–9.
32. Silva AF, Rangel L, Ortiz CG, Morales E, Zanella EL, Castillo-Velázquez U, et al. Increased incidence of DNA amplification in follicular than in uterine and blood samples indicates possible tropism of *Neospora caninum* to the ovarian follicle. Vet Parasitol. 2012;188:175–8.
33. Amdouni Y, Rjeibi MR, Awadi S, Gharbi M. Molecular identification of *Neospora caninum* and co-infection with *Toxoplasma gondii* in genital apparatus of naturally infected cows in North Tunisia. Trop Anim Health Prod. 2021;53:528.
34. Orozco MA, Morales E, Salmerón F. Characterization of the inflammatory response in the uteri of cows infected naturally by *Neospora caninum*. J Comp Pathol. 2013;148:148–56.
35. Zhao SS, Tao DL, Chen JM, Chen X, Geng XL, Wang JW, et al. *Neospora caninum* infection activated autophagy of caprine endometrial epithelial cells via mTOR signaling. Vet Parasitol. 2022;304:109685.
36. Kopylova E, Noé L, Touzet H. SortMeRNA: fast and accurate filtering of ribosomal RNAs in metatranscriptomic data. Bioinformatics. 2012;28:3211–7.
37. Bolger AM, Lohse M, Usadel B. Trimmomatic: a flexible trimmer for Illumina sequence data. Bioinformatics. 2014;30:2114–20.
38. Chen S, Zhou Y, Chen Y, Gu J. Fastp: an ultra-fast all-in-one FASTQ preprocessor. Bioinformatics. 2018;34:i884–90.
39. Kim D, Langmead B, Salzberg SL. HISAT: a fast spliced aligner with low memory requirements. Nat Methods. 2015;12:357–60.
40. Pertea M, Pertea GM, Antonescu CM, Chang TC, Mendell JT, Salzberg SL. StringTie enables improved reconstruction of a transcriptome from RNA-seq reads. Nat Biotechnol. 2015;33:290–5.
41. Sonnhammer EL, Eddy SR, Birney E, Bateman A, Durbin R. Pfam: multiple sequence alignments and HMM-profiles of protein domains. Nucleic Acids Res. 1998;26:320–2.
42. Sun L, Luo H, Bu D, Zhao G, Yu K, Zhang C, et al. Utilizing sequence intrinsic composition to classify protein-coding and long non-coding transcripts. Nucleic Acids Res. 2013;41:e166.
43. Kang YJ, Yang DC, Kong L, Hou M, Meng YQ, Wei L, et al. CPC2: a fast and accurate coding potential calculator based on sequence intrinsic features. Nucleic Acids Res. 2017;45:W12–6.
44. Li A, Zhang J, Zhou Z. PLEK: a tool for predicting long non-coding RNAs and messenger RNAs based on an improved *k*-mer scheme. BMC Bioinform. 2014;15:311.
45. Roberts A, Pachter L. Streaming fragment assignment for real-time analysis of sequencing experiments. Nat Methods. 2013;10:71–73.
46. Wucher V, Legeai F, Hédan B, Rizk G, Lagoutte L, Leeb T, et al. FEELnc: a tool for long non-coding RNA annotation and its application to the dog transcriptome. Nucleic Acids Res. 2017;45:e57.
47. Alkan F, Wenzel A, Palasca O, Kerpedjiev P, Rudebeck AF, Stadler PF, et al. RIsearch2: suffix array-based large-scale prediction of RNA-RNA interactions and siRNA off-targets. Nucleic Acids Res. 2017;45:e60.
48. Li L, Wang XC, Gong PT, Zhang N, Zhang X, Li S, et al. ROS-mediated NLRP3 inflammasome activation participates in the response against *Neospora caninum* infection. Parasit Vectors. 2020;13:449.
49. Jin X, Gong P, Zhang X, Li G, Zhu T, Zhang M, et al. Activation of ERK signaling via TLR11 induces IL-12p40 production in peritoneal macrophages challenged by *Neospora caninum*. Front Microbiol. 2017;8:1393.
50. Yang C, Liu J, Ma L, Zhang X, Zhang X, Zhou B, et al. NcGRA17 is an important regulator of parasitophorous vacuole morphology and pathogenicity of *Neospora caninum*. Vet Parasitol. 2018;264:26–34.
51. Wang J, Tang D, Li W, Xu J, Liu Q, Liu J. A new microneme protein of *Neospora caninum*, NcMIC8 is involved in host cell invasion. Exp Parasitol. 2017;175:21–7.
52. Alaeddine F, Hemphill A, Debache K, Guionaud C. Molecular cloning and characterization of NcROP2Fam-1, a member of the ROP2 family of rhoptry proteins in *Neospora caninum* that is targeted by antibodies neutralizing host cell invasion in vitro. Parasitology. 2013;140:1033–50.
53. Olajide JS, Olopade B, Cai J. Functional intricacy and symmetry of long non-coding RNAs in parasitic infections. Front Cell Infect Microbiol. 2021;11:751523.
54. Li M, Gong AY, Zhang XT, Wang Y, Mathy NW, Martins GA, et al. Induction of a long noncoding RNA transcript, NR_045064, promotes defense gene transcription and facilitates intestinal epithelial cell responses against *Cryptosporidium* infection. J Immunol. 2018;201:3630–40.
55. Liu W, Huang L, Wei Q, Zhang Y, Zhang S, Zhang W, et al. Microarray analysis of long non-coding RNA expression profiles uncovers a *Toxoplasma*-induced negative regulation of host immune signaling. Parasit Vectors. 2018;11:174.
56. Takeuchi O, Akira S. Pattern recognition receptors and inflammation. Cell. 2010;140:805–20.
57. Miranda VDS, França FBF, da Costa MS, Silva VRS, Mota CM, Barros PDSC, et al. Toll-like receptor 3-TRIF pathway activation by *Neospora caninum* RNA enhances infection control in mice. Infect Immun. 2019;87:e00739-e818.
58. Mineo TW, Oliveira CJ, Gutierrez FR, Silva JS. Recognition by Toll-like receptor 2 induces antigen-presenting cell activation and Th1 programming during infection by *Neospora caninum*. Immunol Cell Biol. 2010;88:825–33.
59. Zhang X, Li X, Gong P, Wang X, Zhang N, Chen M, et al. Host defense against *Neospora caninum* infection via IL-12p40 production through TLR2/TLR3-AKT-ERK signaling pathway in C57BL/6 mice. Mol Immunol. 2021;139:140–52.
60. Débare H, Moiré N, Ducournau C, Schmidt J, Laakmann JD, Schwarz RT, et al. *Neospora caninum* glycosylphosphatidylinositols used as adjuvants modulate cellular immune responses induced in vitro by a nanoparticle-based vaccine. Cytokine. 2021;144:155575.
61. Fereig RM, Abdelbaky HH, Kuroda Y, Nishikawa Y. Critical role of TLR2 in triggering protective immunity with cyclophilin entrapped in oligomannose-coated liposomes against *Neospora caninum* infection in mice. Vaccine. 2019;37:937–44.
62. Li S, Gong P, Tai L, Li X, Wang X, Zhao C, et al. Extracellular vesicles secreted by *Neospora caninum* are recognized by toll-like receptor 2 and modulate host cell innate immunity through the MAPK signaling pathway. Front Immunol. 2018;9:1633.
63. Jiménez-Pelayo L, García-Sánchez M, Regidor-Cerrillo J, Horcajo P, Collantes-Fernández E, Gómez-Bautista M, et al. Immune response profile of caruncular and trophoblast cell lines infected by high- (Nc-Spain7) and low-virulence (Nc-Spain1H) isolates of *Neospora caninum*. Parasit Vectors. 2019;12:218.
64. Marin MS, Hecker YP, Quintana S, Pérez SE, Leunda MR, Cantón GJ, et al. Toll-like receptors 3, 7 and 8 are upregulated in the placental caruncle and fetal spleen of *Neospora caninum* experimentally infected cattle. Vet Parasitol. 2017;236:58–61.
65. Marin MS, Hecker YP, Quintana S, Pérez SE, Leunda MR, Cantón GJ, et al. Immunization with inactivated antigens of *Neospora caninum* induces Toll-like receptors 3, 7, 8 and 9 in maternal-fetal interface of infected pregnant heifers. Vet Parasitol. 2017;243:12–7.
66. Wang X, Gong P, Zhang X, Li S, Lu X, Zhao C, et al. NLRP3 inflammasome participates in host response to *Neospora caninum* infection. Front Immunol. 2018;9:1791.
67. Wang X, Gong P, Zhang N, Li L, Chen S, Jia L, et al. Inflammasome activation restrains the intracellular *Neospora caninum* proliferation in bovine macrophages. Vet Parasitol. 2019;268:16–20.
68. Mukherjee T, Hovingh ES, Foerster EG, Abdel-Nour M, Philpott DJ, Girardin SE. NOD1 and NOD2 in inflammation, immunity and disease. Arch Biochem Biophys. 2019;670:69–81.
69. Berraondo P, Sanmamed MF, Ochoa MC, Etxeberria I, Aznar MA, Pérez-Gracia JL, et al. Cytokines in clinical cancer immunotherapy. Br J Cancer. 2019;120:6–15.
70. Yamane I, Kitani H, Kokuho T, Shibahara T, Haritani M, Hamaoka T, et al. The inhibitory effect of interferon gamma and tumor necrosis factor alpha on intracellular multiplication of *Neospora caninum* in primary bovine brain cells. J Vet Med Sci. 2000;62:347–51.
71. Boucher E, Marin M, Holani R, Young-Speirs M, Moore DM, Cobo ER. Characteristic pro-inflammatory cytokines and host defence cathelicidin

peptide produced by human monocyte-derived macrophages infected with *Neospora caninum*. Parasitology. 2018;145:871–84.
72. Baszler TV, Long MT, McElwain TF, Mathison BA. Interferon-gamma and interleukin-12 mediate protection to acute *Neospora caninum* infection in BALB/c mice. Int J Parasitol. 1999;29:1635–46.
73. Maley SW, Buxton D, Macaldowie CN, Anderson IE, Wright SE, Bartley PM, et al. Characterization of the immune response in the placenta of cattle experimentally infected with *Neospora caninum* in early gestation. J Comp Pathol. 2006;135:130–41.
74. Rosbottom A, Gibney EH, Guy CS, Kipar A, Smith RF, Kaiser P, et al. Upregulation of cytokines is detected in the placentas of cattle infected with *Neospora caninum* and is more marked early in gestation when fetal death is observed. Infect Immun. 2008;76:2352–61.
75. Sun Y, Liu WZ, Liu T, Feng X, Yang N, Zhou HF. Signaling pathway of MAPK/ERK in cell proliferation, differentiation, migration, senescence and apoptosis. J Recept Signal Transduct Res. 2015;35:600–4.
76. Korbecki J, Bobiński R, Dutka M. Self-regulation of the inflammatory response by peroxisome proliferator-activated receptors. Inflamm Res. 2019;68:443–58.
77. Sanderson MP, Dempsey PJ, Dunbar AJ. Control of ErbB signaling through metalloprotease mediated ectodomain shedding of EGF-like factors. Growth Factors. 2006;24:121–36.
78. Sukumaran P, Nascimento Da Conceicao V, Sun Y, Ahamad N, Saraiva LR, Selvaraj S, et al. Calcium signaling regulates autophagy and apoptosis. Cells. 2021;10:2125.
79. Ihnatko R, Kubes M. TNF signaling: early events and phosphorylation. Gen Physiol Biophys. 2007;26:159–67.
80. Mihaylova MM, Shaw RJ. The AMPK signalling pathway coordinates cell growth, autophagy and metabolism. Nat Cell Biol. 2011;13:1016–23.
81. Cui J, Liu X, Yang L, Che S, Guo H, Han J, et al. MiR-184 combined with STC2 promotes endometrial epithelial cell apoptosis in dairy goats via RAS/RAF/MEK/ERK pathway. Genes (Basel). 2020;11:1052.
82. Lai R, Ji L, Zhang X, Xu Y, Zhong Y, Chen L, et al. Stanniocalcin 2 inhibits the epithelial-mesenchymal transition and invasion of trophoblasts via activation of autophagy under high-glucose conditions. Mol Cell Endocrinol. 2022;547:111598.
83. Wang J, Wang X, Gong P, Ren F, Li X, Zhang N, et al. The protective role of TLR2 mediates impaired autophagic flux by activating the mTOR pathway during *Neospora caninum* infection in mice. Front Cell Infect Microbiol. 2021;11:788340.
84. Mota CM, Oliveira ACM, Davoli-Ferreira M, Silva MV, Santiago FM, Nadipuram SM, et al. Corrigendum: *Neospora caninum* activates p38 MAPK as an evasion mechanism against innate immunity. Front Microbiol. 2019;10:548.
85. Jin X, Gong P, Li G, Zhang X, Li J. The p38 MAPK inhibitor, SB203580, inhibits cell invasion by *Neospora caninum*. Parasitol Res. 2017;116:813–9.
86. Zhang L, An XP, Liu XR, Fu MZ, Han P, Peng JY, et al. Characterization of the transcriptional complexity of the receptive and pre-receptive endometria of dairy goats. Sci Rep. 2015;5:14244.
87. Achache H, Revel A. Endometrial receptivity markers, the journey to successful embryo implantation. Hum Reprod Update. 2006;12:731–46.

Publisher's Note